

Evolutionary History of the South American Mistletoe *Tripodanthus* (Loranthaceae) Using Nuclear and Plastid Markers

Guillermo C. Amico,^{1,4} Romina Vidal-Russell,¹ Miguel A. Garcia,² and Daniel L. Nickrent³

¹Laboratorio Ecotono, INIBIOMA (CONICET-Universidad Nacional del Comahue) Quintral 1250, 8400 Bariloche, Río Negro, Argentina.

²Real Jardín Botánico, CSIC, Plaza de Murillo 2, 28014 Madrid, Spain.

³Department of Plant Biology, Southern Illinois University Carbondale, Illinois 62901-6509, U. S. A.

⁴Author for correspondence (guillermo.amico@conicet.gov.ar)

Communicating Editor: Lúcia Lohmann

Abstract—*Tripodanthus* consists of three species that are endemic to South America. While *T. acutifolius* and *T. flagellaris* have east-west distributions in tropical and subtropical South America, *T. belmirensis* is restricted to its type locality in the region of Belmira, Colombia. The objective of the present study was to reconstruct the phylogeny of the genus using molecular markers (nrDNA ITS and plastid *atpB-rbcL* and *trnL-F* regions) and to examine morphological characters in the variable species *T. acutifolius*. A total of 23 individuals of *Tripodanthus*, representing all species currently recognized in the genus, were sampled in the molecular phylogeny, while 73 individuals were measured for the morphological component of this study. Phylogenetic analyses of the combined ITS and plastid markers reconstructed two main clades within *T. acutifolius* that correspond to two geographic areas: the Andes and the eastern region of southern South America. This analysis also yielded a monophyletic *T. flagellaris*, although no geographic structure was obtained within this clade. *Tripodanthus belmirensis* and *T. acutifolius* together formed a clade that was sister to *T. flagellaris*. A principal component analysis of 70 individuals of *T. acutifolius* showed great variability in leaf morphological characters, leading to overlapping clusters for Andean and eastern mistletoes. The morphologically variable *T. acutifolius* was not well supported as monophyletic and possessed overlapping morphological features with *T. belmirensis*, calling into question whether *T. belmirensis* should be recognized as a distinct species.

Keywords—Amphiphagy, Andes, Brazil, biogeography, host plant, parasitic plant, Santalales.

Loranthaceae includes approximately 73 genera and 915 species (Nickrent et al. 2010), representing the largest mistletoe family. Time-calibrated phylogenies (chronograms) have shown that Loranthaceae arose in the Cretaceous (as root parasites) and diversified (as stem parasites) during the Oligocene (Vidal-Russell and Nickrent 2008a). Of the 73 genera currently recognized in the family, 16 occur in South America and, except for *Gaiadendron* G. Don, form a monophyletic group (Vidal-Russell and Nickrent 2008b). The earliest diverging members of this South American clade possess base chromosome numbers of $x = 12$ (*Notanthera* G. Don and *Tristerix* Mart.), $x = 10$ (*Ligaria* Tiegh.), and $x = 16$ (*Desmaria* Tiegh.), whereas all the remaining genera are $x = 8$. *Tripodanthus*, with $x = 8$ is sister to the other ten $x = 8$ genera (Vidal-Russell and Nickrent 2008b).

Tripodanthus consists of three species, *T. acutifolius* Tiegh., *T. flagellaris* Tiegh., and *T. belmirensis* Roldán & Kuijt, endemic to South America. Four additional species have been described, *T. eugenioides* Tiegh., *T. destructor* Tiegh., *T. ligustrinus* Tiegh., and *T. suaveolens* Tiegh.; however, these are now considered synonyms of *T. acutifolius* (Barlow and Wiens 1973; Kuijt 1986).

Tripodanthus acutifolius has a disjunct distribution in South America (Fig. 1). In the eastern region it is found in north-eastern Argentina, Uruguay, and south-central Brazil, whereas in the west it is present in the Guiana Highlands (Venezuela), as well as in the Andean region from Ecuador to northwestern Argentina, extending east to Bolivia and Paraguay. The Chaco biome separates the eastern populations from the Andean populations. It is unknown whether *Tripodanthus acutifolius* occurs in Colombia. The other two species have narrower distributions. *Tripodanthus flagellaris* is found in the Andes of northwestern Argentina, the Sierras Centrales of Argentina, and in northeastern Argentina, Uruguay, and south-central Brazil (eastern region). This species

occurs sympatrically with *T. acutifolius* in two regions, the Andes of northwestern Argentina and in the eastern portions of Argentina (Abbiatti 1946) (Fig. 1). *Tripodanthus belmirensis* is restricted to Belmira, Antioquia, Colombia, the type locality (Roldán and Kuijt 2005). In general, *Tripodanthus* species are found at high elevations (> 1,000 m) in the Andes, but at low elevations in the eastern portions of South America.

Morphologically, *Tripodanthus* is characterized by hexamerous flowers, with isomorphic stamens, and versatile anthers. *Tripodanthus acutifolius* and *T. flagellaris* have fragrant, small (1–1.5 cm), short-tubular, white to light yellow or pink flowers, while *T. belmirensis* has larger (3 cm) bright red flowers. Some individuals of *T. acutifolius* may also have flowers that reach 3 cm in length. *Tripodanthus acutifolius* and *T. flagellaris* also possess epicortical roots, as do other South American Loranthaceae genera (not known for *T. belmirensis*). As with most Loranthaceae, *Tripodanthus* is a stem parasitic plant, but *T. acutifolius* may also be amphiphagous sensu Der and Nickrent (2008). For this trophic mode, some individuals parasitize aerial parts of the host and then, via epicortical roots, grow down the host stem to the ground where they form secondary haustorial connections to host roots. The other two species in the genus have not been documented to be root parasites. *Tripodanthus flagellaris* is a clambering stem parasite and *T. belmirensis* is a shrubby stem parasite (Abbiatti 1946; Thoday 1961; Roldán and Kuijt 2005).

The main objective of the present study was to reconstruct relationships within *Tripodanthus* using molecular markers. We also wanted to determine whether clades within the two disjunct species, *T. acutifolius* and *T. flagellaris*, are geographically structured. In addition, we wanted to test the monophyly of *T. acutifolius*, the species with widest distribution and most variable morphology. Leaf morphological characters were examined in *T. acutifolius* to determine whether patterns of

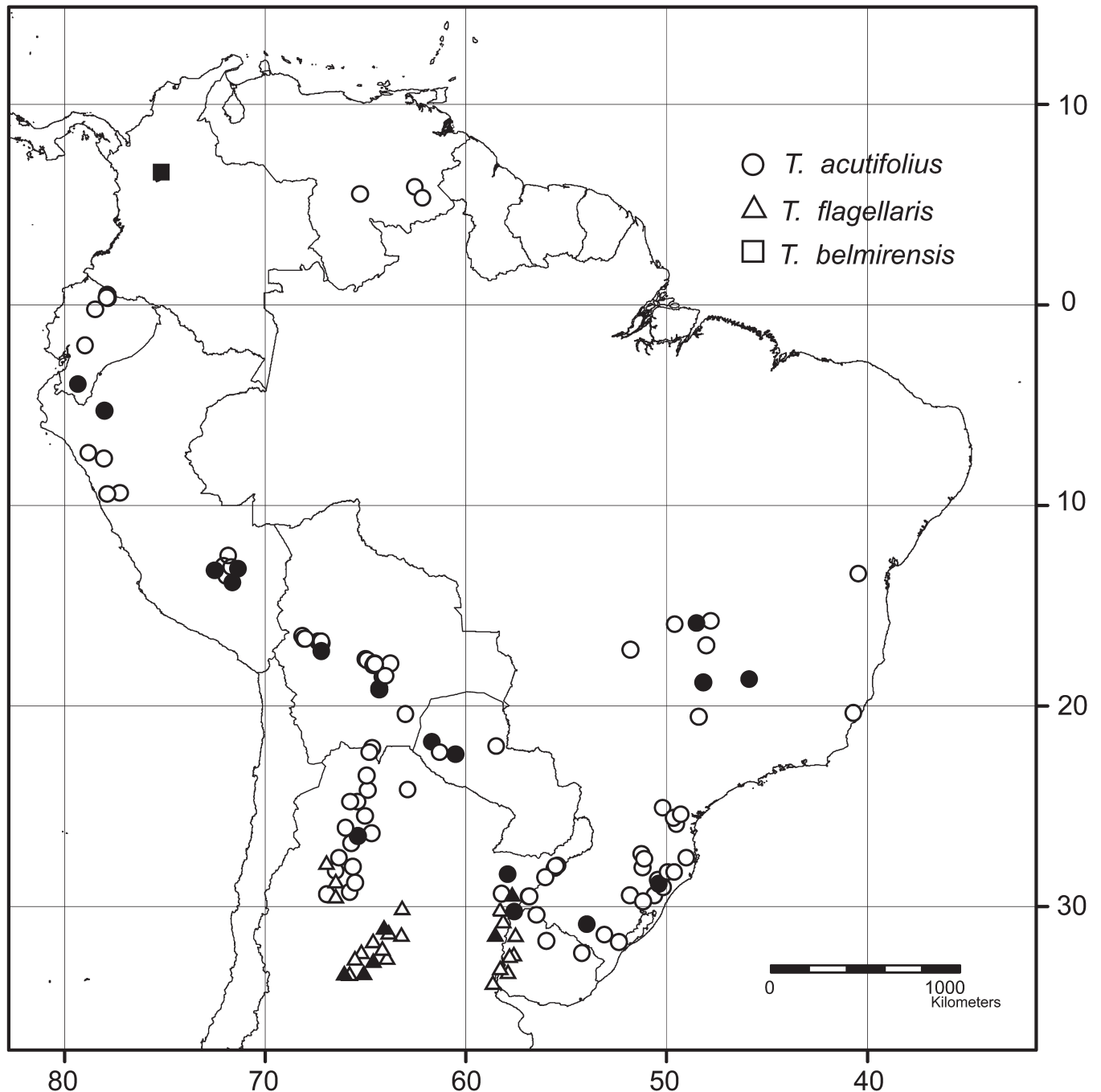


FIG. 1. Geographical distribution of *Tripodanthus* based on herbarium specimens. Filled symbols represent the accessions used in this study.

variation exist, and if so, whether these morphotypes correlate with clades determined from the molecular analyses.

MATERIALS AND METHODS

Taxon Sampling for the Molecular Phylogenetic Study—A total of 23 individuals of *Tripodanthus* representing all three species currently recognized in the genus were sampled (Fig. 1, Appendix 1). A more intensive sampling scheme was used for *T. acutifolius* to test the monophyly of this morphologically variable and widely distributed species. Individuals from 16 localities representing six of the seven countries in which this species occurs were sampled (no samples from Venezuela). *Desmaria mutabilis* (Poepp. & Endl.) Tiegh. ex T. Durand & B. D. Jacks., *Ligaria cuneifolia* (Ruiz & Pav.) Tiegh., *Notanthera heterophylla* (Ruiz & Pav.)

G. Don, and *Tristerix chodatianus* (Patschovsky) Kuijt were selected as outgroups based on Vidal-Russell and Nickrent (2008b).

DNA Extraction, Amplification, and Sequencing—DNA was extracted from silica-dried or herbarium specimens using either a 2 × CTAB method (Nickrent 1994) or the DNeasy plant mini kit (QiaGen, Valencia, California). Typical PCR amplification reactions included 1 × Promega buffer (Madison, Wisconsin) (10 mM Tris HCl, 50 mM KCl, pH 8.3), 1.5 mM MgCl₂, 50 μM dNTPs, 1 unit *Taq* polymerase, 0.4 μM of each primer, and ca. 30 ng of genomic DNA. In some cases PCR reactions were prepared in 25 μl volumes using PuReTaq™ Ready-to-Go™ PCR beads (GE Healthcare, Little Chalfont, U. K.). The *atpB-rbcL* and the *trnL-trnF* intergenic spacers were amplified and sequenced using primers described in Amico et al. (2007) and Taberlet et al. (1991). In addition, the ITS region was amplified and sequenced using the primer pair 18S 1830 forward and 26S 40 reverse (Amico et al. 2007).

The PCR thermal cycling conditions for the plastid regions used a touch down profile: 5 min at 95°C, 5 cycles of 30 sec at 94°C, 30 sec at 52°C, and 1 min at 72°C, followed by 33 cycles of 30 sec at 94°C, 30 sec at 48°C, and 1 min at 72°C, with a final extension of 10 min at 72°C. For ITS, cycling conditions were as follows: 5 min at 95°C, 35 cycles of 1 min at 94°C, 1 min at 52°C, and 1 min at 72°C, with a final extension of 10 min at 72°C. Negative controls that lacked genomic DNA were included to check for DNA contamination. Cycle sequencing reactions were performed directly on the purified PCR products following standard protocols using BigDye terminator cycle sequencing ready reaction kit with AmpliTaq DNA polymerase (Applied Biosystems, Foster City, California) with better buffer (The Gel Company, San Francisco, California). Some sequences were obtained at Southern Illinois University using an ABI 377 automated sequencer (Applied Biosystems) and others sent to Macrogen, Inc. (Seoul, South Korea).

Phylogeny Reconstruction—Sequences were aligned manually using the computer program BioEdit version 7.0.9 (Hall 1999). The alignment contained several gaps that were unambiguously aligned. Indels for the plastid partitions provided phylogenetic information and were coded separately as present or absent. In contrast, indels in the ITS data set were not informative, and were treated as missing data. Gaps were considered homologous only when they shared identical boundaries and length. All data matrices were deposited in TreeBASE (study number S10347).

We used maximum parsimony (MP), maximum likelihood (ML) and Bayesian inference (BI) to estimate evolutionary relationships among taxa. Incongruence length tests (ILD) with 500 replicates were performed in PAUP* version 4.01b10 (Swofford 2002) to determine potential conflict between the individual data sets. Maximum parsimony and ML analyses were conducted in PAUP* while BI analyses were conducted in MrBayes version 3.1.2 (Ronquist and Huelsenbeck 2003). Heuristic MP searches with TBR branch swapping were conducted for the individual and combined data sets. Nodal support was assessed through nonparametric bootstrap (MPBS) (Felsenstein 1985), which used 100 pseudoreplicates and the same settings used in the original search. Indels were manually coded as "A" or "T" in the MP analyses. Models of sequence evolution for each data partition were determined by the hierarchical likelihood ratio test using Modeltest version 3.6 (Posada and Crandall 1998) and MrModeltest version 2 (Nylander et al. 2004). For each plastid region, the K81uf + G was used in ML searches and GTR + G in BI searches, TrN + G was used in the ML and GTR + G in the BI of the nuclear data set. When all three partitions were combined, ML searches were performed with RAxML (Stamatakis 2006) using a partition scheme with a GTR + G model of DNA substitution. Support was assessed using 1,000 bootstrap replicates and the same settings used in the original search. Individual ML analyses were conducted in PAUP* with the models mentioned above. Heuristic searches were performed using a neighbor joining tree as a starting tree and TBR as the swapping algorithm. Nodal support was obtained using nonparametric bootstrap with 100 pseudoreplicates (MLBS). Bayesian searches included two independent analyses, each with four chains, and run for five million generations. The run was set to stop when topological convergence was reached between the two runs, which was determined by the presence of a standard deviation in split frequencies that was lower than 0.01 (discarding 25% as burn-in). For BI, indels were manually coded as "0" or "1" and treated as restriction data in a mixed matrix input file. Trees and parameters were saved every 100 generations. Starting model parameters were assigned a uniform prior probability distribution except for the base frequencies where a Dirichlet distribution was assigned. Parameters were estimated as part of the analyses, but the estimates between them were unlinked in cases where both partitions were analyzed, allowing each run to vary independently.

Morphological Analyses—Photographs of herbarium specimens from MO, CTES, and HUA were used to construct a leaf morphological data set for *T. acutifolius* and *T. belmirensis*. A total of 73 individuals were sampled, 70 represented *T. acutifolius* and three represented *T. belmirensis*. Samples of *T. acutifolius* included 30 individuals from the eastern region, 36 from the western Andean region, and four from the Guiana Highlands. The leaf photographs were analyzed using the image analysis software package Digimizer v. 3.7.0 (MedCalc Software, Mariakerke, Belgium). Calibration was achieved using a ruler that was photographed simultaneously with each specimen. For each individual, at least three undamaged and fully expanded leaves were selected and measured (total $n = 293$). In total, five morphological variables were used: area, perimeter, length, width, and roundness. Normality for each variable was examined using the Shapiro-Wilk test. Because all variables deviated from normality, measurements were \log^{-10} transformed. Morphological

variables (\log^{-10} transformed) were analyzed using principal component analysis (PCA, JMP Version 7, SAS Institute Inc., Cary, North Carolina), and eigen-values extracted from the variance/covariance matrix.

RESULTS

Sequence alignment length and the general statistics derived from the parsimony analyses are presented in Table 1. Sequences of the *atpB-rbcL* spacer were not obtained from three accessions of *T. acutifolius* and three accessions of *T. flagellaris*. ITS sequences were lacking for two accessions of *T. acutifolius*. All *atpB-rbcL* sequences of *T. flagellaris* possessed the same haplotype, and all sequences of *T. acutifolius* from Challabamba, Ollantaytambo, and Tapia possessed the same haplotype.

A total of seven indels were coded for *atpB-rbcL* and two for *trnL-F*. For the *atpB-rbcL* spacer, all individuals of *T. acutifolius* from the Andean region shared a deletion of 121 bp.; two shorter indels characterized accessions from the eastern region and one was present in two individuals from Bolivia and one from Paraguay. In *T. flagellaris*, three indels were found in the *atpB-rbcL* spacer and two in *trnL-F*.

Phylogenetic Analyses of the Plastid Data—The topologies that resulted from the analysis of each independent plastid region (*atpB-rbcL*, *trnL-F*) were not significantly incongruent based on the ILD test ($p < 1.0$), thus these partitions were combined into a single matrix and analyzed jointly. Analyses of the plastid data set recovered a monophyletic *T. flagellaris* (MPBS = 100, MLBS = 100, Posterior probability (PP) = 1.00; Fig. 2A). Conversely, *T. acutifolius* was not supported as monophyletic with *T. flagellaris* and *T. belmirensis* nested within it. Constraining *T. acutifolius* as monophyletic gave a tree four steps longer, but based on the Wilcoxon signed-ranks test (Templeton 1983) or the winning-sites test (Prager and Wilson 1988), it was not significantly longer. The geographically separated localities of *T. acutifolius* (eastern and Andean regions) form two well-supported clades with high bootstrap and BI posterior probability scores (eastern region: MPBS = 94, MLBS = 98, PP = 1.00; Andean region: MPBS = 87, MLBS = 87, PP = 1.00; Fig. 2A).

Phylogenetic Analyses of the Nuclear Data Set—Analyses of the ITS data set recovered two major clades (Fig. 2B): a *Tripodanthus flagellaris* clade (MPBS = 100, MLBS = 100, PP = 1.00) and a clade including *T. acutifolius* and *T. belmirensis* (MPBS = 100, MLBS = 64, PP = 0.54). Monophyly of *T. acutifolius* received low support (MPBS = 61, PP = 0.75). Within *T. acutifolius*, relationships among individuals were similar to those recovered based on the plastid partition. In particular, an eastern clade received high BI support (PP = 0.97) and was sister to a clade represented by two monophyletic

TABLE 1. Summary statistics derived from the phylogenetic analyses of the molecular data sets. PIC = parsimony informative characters; CI = consistency index; RI = retention index.

Partition	Aligned length	PIC	Trees	Tree Length	CI	RI
<i>trnL-F</i>	667	33	66	125	0.84	0.84
<i>atpB-rbcL</i>	706	33	60	125	0.94	0.92
<i>trnL-F</i> + <i>atpB-rbcL</i>	1,381	72	83,928	258	0.89	0.88
ITS	771	126	12	393	0.83	0.87
All	2,153	198	2,496	662	0.84	0.86

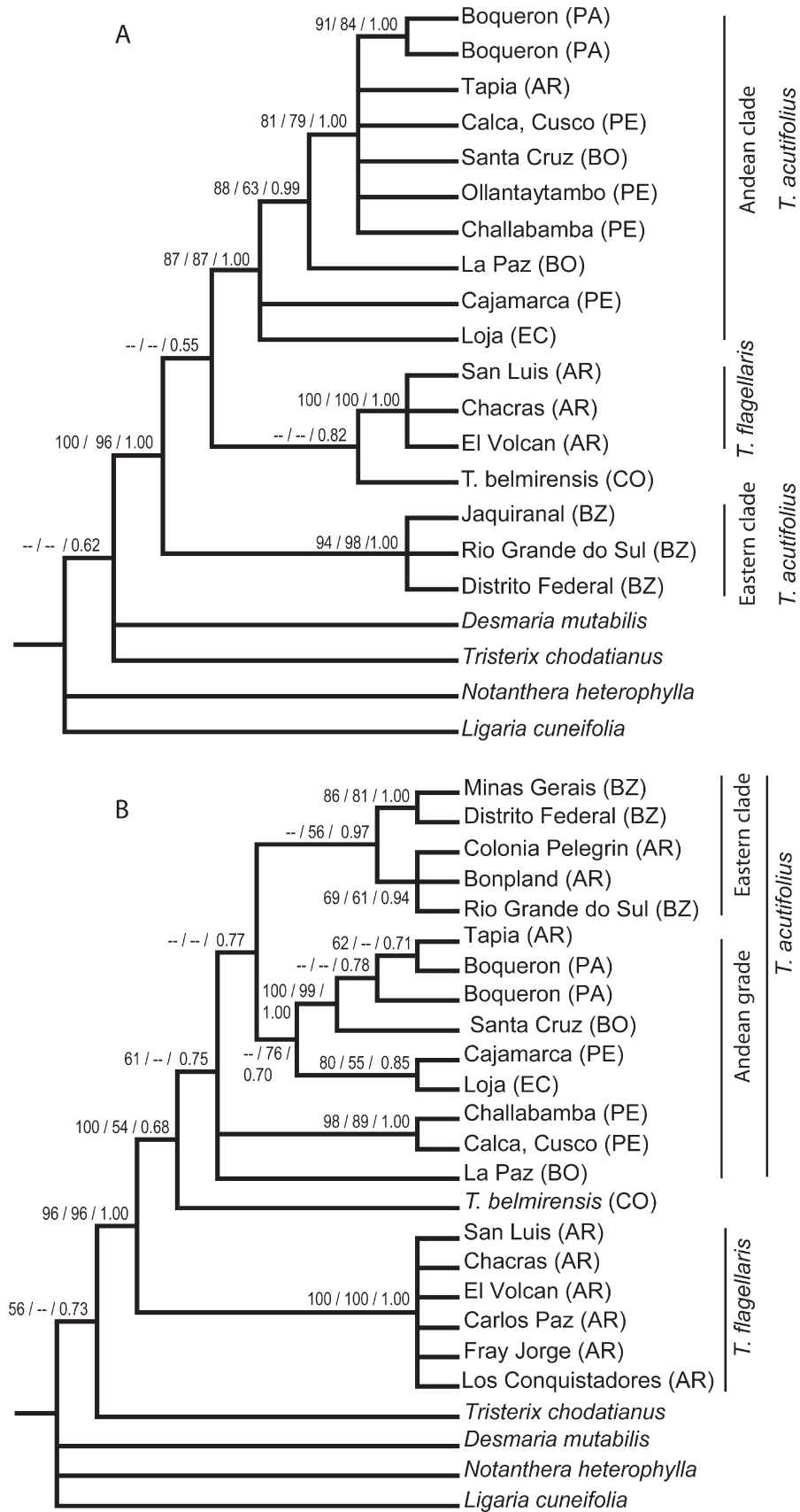


FIG. 2. Bayesian consensus topologies resulting from the analyses of the combined plastid partitions (A) and nuclear ribosomal ITS data (B) for *Tripodanthus* species. Numbers at the nodes represent maximum parsimony bootstrap values (1,000 pseudoreplicates), maximum likelihood bootstrap values (100 pseudoreplicates), and Bayesian posterior probabilities.

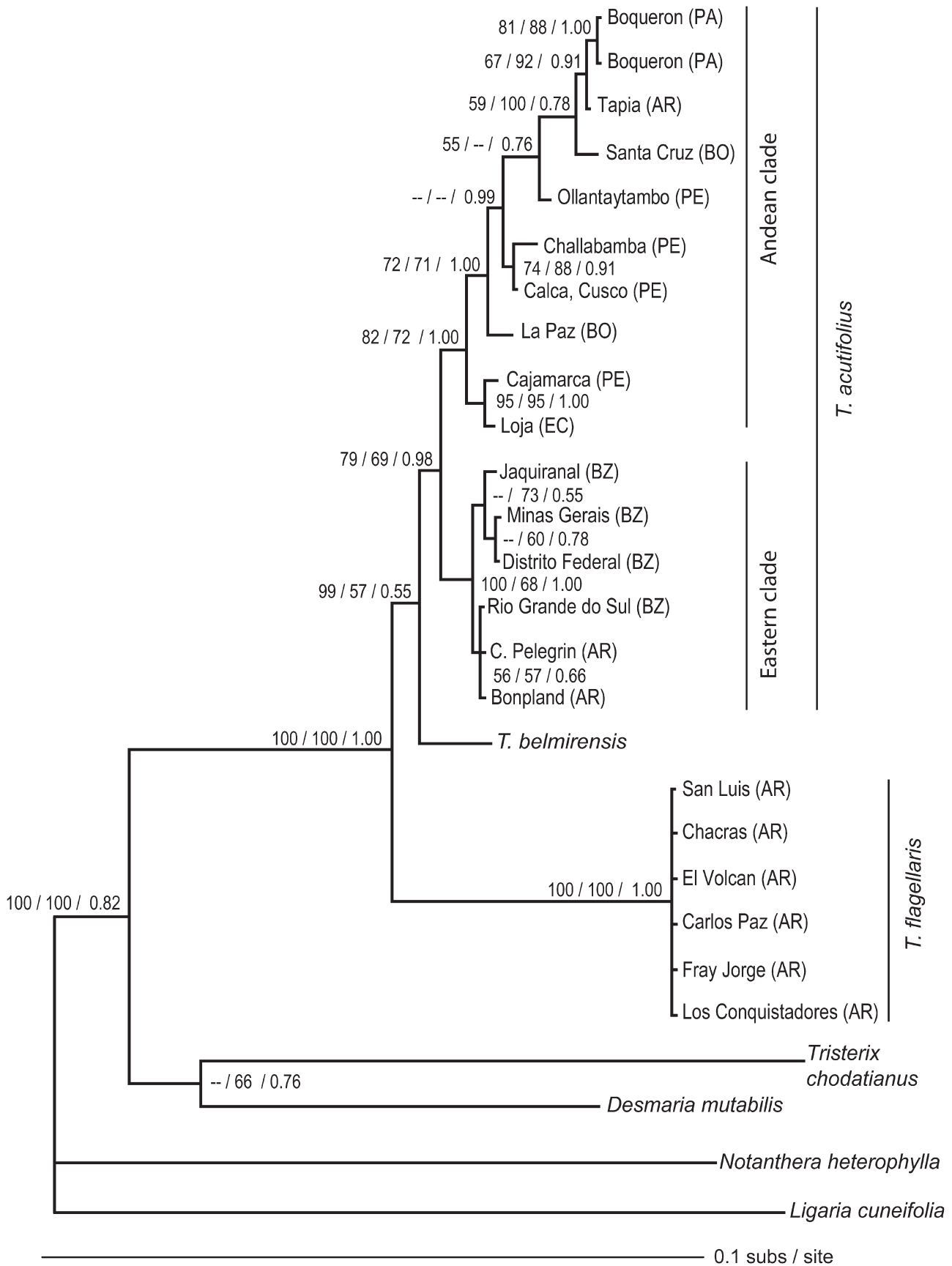


FIG. 3. Phylogram derived from a Bayesian analysis of the combined plastid and nuclear partitions. Numbers at the nodes represent maximum parsimony (MP) bootstrap values (1,000 pseudoreplicates), maximum likelihood (ML) bootstrap values (1,000 pseudoreplicates), and Bayesian posterior probabilities.

groups: one with accessions from Boquerón (Paraguay), Santa Cruz (Bolivia), and Northwest Argentina, and the other with accessions from Cajamarca (northern Peru) and Loja (Ecuador). An accession from Bolivia (La Paz), a clade of two accessions from Peru (Challabamba and Calca) and a clade composed of the remaining *T. acutifolius* accessions formed a polytomy.

Combined Molecular Analyses—The analyses of a combined molecular data set produced a topology that was generally congruent with the topologies derived from the analyses of the individual partitions and also showed increased overall support for the relationships recovered (Table 1, Fig. 3). A monophyletic *Tripodanthus* (MPBS = 100, MLBS = 100, PP = 1.00) was recovered, with *T. flagellaris* also strongly supported as monophyletic (MPBS = 100, MLBS = 100, PP = 1.00) and sister to a clade composed of *T. belmirensis* and *T. acutifolius*. A monophyletic *T. acutifolius* (MPBS = 79, MLBS = 69, PP = 0.98) was composed of two main clades, an Andean clade (MPBS = 82, MLBS = 72, PP = 1.00) and an eastern clade (MPBS = 100, MLBS = 98, PP = 1.00). Within the Andean clade, the accessions from Ecuador (Loja) and northern Peru (Cajamarca) formed a clade that was sister to the remaining Andean accessions.

Morphological Analysis—Overall results derived from a PCA of leaf traits are presented in Fig. 4. Principal components 1 and 2 explained 91.8 and 7.4% of the total variance for the \log^{-10} transformed data. For the most part, the Andean (western) individuals clustered on one side of the graph, while the eastern individuals clustered on the opposite side; however, the overall point distributions of both overlapped. Thus, the two groups of *T. acutifolius* that were clearly defined by the molecular phylogeny were not seen using leaf morphology. In particular, the accessions of *T. acutifolius* from the Guiana Highlands, and those of *T. belmirensis* from Colombia, were not differentiated from the remaining accessions of *T. acutifolius*. However, the three individuals of *T. belmirensis* sampled formed a tight cluster within the overall morphospace of *T. acutifolius* (Fig. 4).

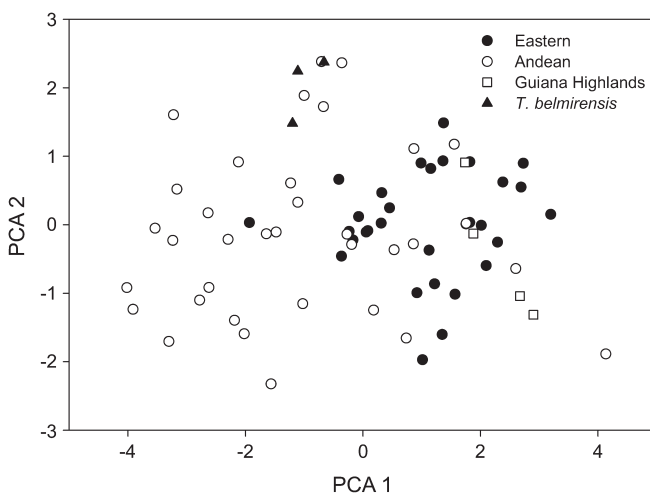


FIG. 4. Principal component analysis of five morphological variables obtained from the leaves of *Tripodanthus acutifolius* and *T. belmirensis*. For *T. acutifolius*, black circles represent individuals from the eastern part of South America, white circles represent individuals from the Andean region, and white squares represent individuals from the Guiana Highlands of Venezuela. Black triangles represent individuals of *T. belmirensis*.

DISCUSSION

Phylogeny and Biogeography—Nuclear and plastid gene trees both support the monophyly of the South American mistletoe genus *Tripodanthus*. Within the genus, *T. flagellaris* is also supported as monophyletic and *T. acutifolius* differentiates into two clades that correspond to geographic areas. This study represents the second molecular phylogenetic study to examine interspecific relationships within a genus of Loranthaceae. Similar to Amico et al. (2007), which focused on *Tristerix* and demonstrated the existence of two clades that correlated with a north-south biogeographic pattern, the present study of *Tripodanthus* shows an east-west distribution pattern. *Tripodanthus acutifolius* is differentiated into two major clades: one composed of accessions from the Andean region, and a second that includes accessions from the eastern region of South America (Fig. 3). This species is morphologically diverse, possessing a wide array of flower sizes, flower colors, and nutritional modes. However, these morphological changes do not correlate with geography or the patterns of genetic differentiation recovered from the analyses of the nuclear and plastid markers.

The tree derived from the analysis of the combined molecular data set (Fig. 3) showed that *T. flagellaris* is strongly supported as monophyletic and sister to the other two species included in the genus (*T. acutifolius* and *T. belmirensis*). *Tripodanthus flagellaris* is also morphologically different from the other two species. In particular, its leaves are narrow with an imperfect acrodromous venation pattern (Varela et al. 2008) whereas the other two species possess pinnate venation (Roldán and Kuijt 2005; Varela et al. 2008). Nevertheless, the leaves of *T. flagellaris* have a thin epidermal cuticle and lack lysigenous cavities in the lower epidermis, features that are also present in *T. acutifolius* (Sosa 2003). *Tripodanthus flagellaris* is a clambering mistletoe with prehensile adventitious roots, a habit that is not seen in the other two species. Accessions of *T. flagellaris* from the Sierras Centrales are separated from those in eastern Argentina by 500 km, yet these mistletoes are not genetically differentiated, at least with the markers employed in this study. No accessions of *T. flagellaris* from the Andean region were sampled in the present study, preventing an evaluation of their degree of genetic differentiation. However, given that the Sierras Centrales and Andean regions are linked by a series of highlands, it is possible that no genetic structure exists between these two areas.

We considered that some of the genetic structure found in *Tripodanthus* might be associated with the distribution of its host species. *Tripodanthus flagellaris* grows exclusively on species of Fabaceae (i.e. *Prosopis* and *Acacia* species), those of which have a distribution pattern that is similar to their mistletoe parasite. In contrast, *T. acutifolius* has been reported to parasitize additional genera in Fabaceae as well as members of other plant families such as Anacardiaceae, Myrtaceae, Rosaceae, and Salicaceae. Some of these host species show the same disjunct distribution patterns observed in *T. acutifolius*, particularly in the dry seasonal forests of South America (Prado and Gibbs 1993). The differentiation of the two clades of *T. acutifolius* recovered in the present study might be associated with the same evolutionary forces that have shaped the distribution patterns of their hosts. These distributions are known to have been wider during the last glacial period, and subsequently contracted, thus resulting in the disjunct patterns currently seen (Prado and Gibbs 1993).

When *T. belmirensis* was first described (Roldán and Kuijt 2005), the authors considered a close relationship between this species and representatives of genera such as *Gaiadendron* (based on habitat specificity and floral bracts) and *Tristerix* (based on the red flowers and the presence of acute prophylls). However, the presence of triads in the inflorescence, dimorphic stamens, and pollen characteristics led the authors to place *T. belmirensis* in *Tripodanthus*. Although our molecular study supports placement of this species in *Tripodanthus*, its monophyly is not well supported. Moreover, the analyses of leaf morphological characters were insufficient to distinguish *T. belmirensis* from *T. acutifolius*. These results raise doubts as to whether *T. belmirensis* should indeed be recognized as a new species or whether it should simply be recognized as a morphological variant of the widespread *T. acutifolius*. Nevertheless, a more detailed analysis of *T. belmerensis* and *T. acutifolius*, based on a greater number of specimens, morphological traits, and molecular markers is needed to fully characterize the patterns of genetic and morphological variation found in both of these taxa.

Future studies should focus on the phylogeography of the three species in the genus. In particular, studies using faster molecular markers should provide finer resolution of the genetic structure in the genus, allowing a test of hypotheses associated with potential factors that may limit the distribution of these mistletoes (e.g. host and abiotic factors). *Tripodanthus acutifolius* is one of the few mistletoes to exhibit amphiphagy (root parasitic, stem parasitic, or both), thus representing a potential model for studies on the evolution of trophic modes in mistletoes.

ACKNOWLEDGMENTS. We thank F. Roldán for plant material and photographs, and the herbaria CTES, CORD, HUA, MA, MO, and SI for allowing us to sample materials derived from their collections. Thanks to S. Sipes (SIUC) who allowed us to use her DNA sequencer. We also thank Cecilia Ezcurra, two anonymous reviewers and the editors for useful comments on previous versions of this manuscript. Financial support was provided by the National Science Foundation (to DLN) and the Spanish Consejo Superior de Investigaciones Científicas (CGL2006-00300/BOS to MAG). GCA and RVR are career researchers of the Consejo Nacional de Investigaciones Científicas y Tecnológicas of Argentina (CONICET).

LITERATURE CITED

- Abbiatti, D. 1946. Las Lorantáceas Argentinas. *Revista del Museo de La Plata. Sección Botánica* 7: 1–110.
- Amico, G. C., R. Vidal-Russell, and D. Nickrent. 2007. Phylogenetic relationships and ecological speciation in the mistletoe *Tristerix* (Loranthaceae): the influence of pollinators, dispersers, and hosts. *American Journal of Botany* 94: 558–567.
- Barlow, B. A. and D. Wiens. 1973. The classification of the generic segregates of *Phrygilanthus* (= *Notanthera*) of the Loranthaceae. *Brittonia* 25: 26–39.
- Der, J. P. and D. L. Nickrent. 2008. A molecular phylogeny of Santalaceae (Santalales). *Systematic Botany* 33: 107–116.
- Felsenstein, J. 1985. Confidence limits on phylogenies: an approach using the bootstrap. *Evolution* 39: 783–791.
- Hall, T. A. 1999. BioEdit: a user-friendly biological sequence alignment editor and analysis program for Windows 95/98/NT. *Nucleic Acids Symposium Series* 41: 95–98.
- Kuijt, J. 1986. Loranthaceae. Pp. 113–194 in *Flora of Ecuador* 24, eds. G. Harling and B. Sparre. Stockholm; Riksmuseum, University of Göteborg.
- Nickrent, D. L. 1994. From field to film: rapid sequencing methods for field-collected plant species. *BioTechniques* 16: 470–475.
- Nickrent, D. L., V. Malécot, R. Vidal-Russell, and J. P. Der. 2010. A revised classification of Santalales. *Taxon* 59: 538–558.
- Nylander, J. A. A., F. Ronquist, J. P. Huelsenbeck, and J. L. Nieves-Aldrey. 2004. Bayesian phylogenetic analysis of combined data. *Systematic Biology* 53: 47–67.
- Posada, D. and K. A. Crandall. 1998. MODELTEST: testing the model of DNA substitution. *Bioinformatics* 14: 817–818.
- Prado, D. E. and P. E. Gibbs. 1993. Patterns of species distributions in the dry seasonal forests of South America. *Annals of the Missouri Botanical Garden* 80: 902–927.
- Prager, E. M. and A. C. Wilson. 1988. Ancient origin of lactalbumin from lysozyme: analysis of DNA and amino acid sequences. *Journal of Molecular Evolution* 27: 326–335.
- Roldán, F. J. and J. Kuijt. 2005. A new red-flowered species of *Tripodanthus* (Loranthaceae) from Colombia. *Novon* 15: 207–209.
- Ronquist, F. and J. P. Huelsenbeck. 2003. MrBayes 3: Bayesian phylogenetic inference under mixed models. *Bioinformatics* 19: 1572–1574.
- Sosa, M. M. 2003. *Anatomía foliar de Loranthaceae (sensu lato)*. Resumen B-026, Corrientes, Argentina: Universidad Nacional del Nordeste, Comunicaciones Científicas y Tecnológicas.
- Stamatakis, A. 2006. RAxML-VI-HPC: maximum likelihood-based phylogenetic analyses with thousands of taxa and mixed models. *Bioinformatics* 22: 2688.
- Swofford, D. L. 2002. PAUP*: phylogenetic analysis using parsimony (* and other methods), version 4. Sunderland: Sinauer Associates.
- Taberlet, P., L. Gielly, G. Pautou, and J. Bouvet. 1991. Universal primers for amplification of three noncoding regions of chloroplast DNA. *Plant Molecular Biology* 17: 1105–1109.
- Templeton, A. R. 1983. Phylogenetic inference from restriction endonuclease cleavage site maps with particular reference to the evolution of humans and the apes. *Evolution* 37: 221–244.
- Thoday, D. 1961. Modes of union between parasite and host in Loranthaceae. VI. A general survey of the Loranthoideae. *Proceedings of the Royal Society of London. Series B. Biological Sciences* 155: 1–25.
- Varela, B. G., K. A. Borri, M. J. Ganopol, and A. A. Gurni. 2008. Aplicación del índice de estomas y de la diafanización foliar en la identificación de especies de muérdagos argentinos pertenecientes a Loranthaceae. *Latin American Journal of Pharmacy* 27: 28–33.
- Vidal-Russell, R. and D. L. Nickrent. 2008a. The first mistletoes: origins of aerial parasitism in Santalales. *Molecular Phylogenetics and Evolution* 47: 523–537.
- Vidal-Russell, R. and D. L. Nickrent. 2008b. Evolutionary relationships in the showy mistletoe family (Loranthaceae). *American Journal of Botany* 95: 1015–1029.

APPENDIX 1. Taxon sampling and GenBank accession numbers for *Tripodanthus*. Data are presented in the order of Location, Country, Latitude, Longitude, Elevation, Collector, Herbaria, DNA No., and GenBank numbers for *trnL-F*, *atpB-rbcL*, and ITS. An asterisk indicates an accession number is yet to be assigned.

***T. acutifolius* Tiegh.**: Loja, Loja, Ecuador, 3° 59' 52" S, 79° 18' 38" W, 2100, G. P. Lewis & M. B. Klitgaard 2408, MO 3086585, 5323, HM010433, HM010453, HM010411; Contumaza, Cajamarca, Peru, 7° 25' 00" S, 78° 46' 60" W, 2050, M. O. Dillon & A. Saqástegui 6068, MO 3085711, 5321, HM010432, HM010452, HM010410; Challabamba, Cusco, Peru, 13° 12' 19" S, 71° 38' 35" W, 3200, R. Vidal-Russell & G. C. Amico 51, USM*, 4983, HM010425, HM010447, HM010404; Ollantaytambo, Cusco, Peru, 13° 15' 52" S, 72° 15' 57" W, 1300, R. Vidal Russell 50, USM*, 4927, EU544513, HM010447, Missing; Calca, Cusco, Peru, 13° 19' 25" S, 71° 57' 42" W, 2900, C. Franquemont & E. Franquemont 207, MO 3481724, 4998, HM010426, HM010448, HM010405; Distrito Federal, Distrito Federal, Brazil, 15° 46' 34" S, 47° 47' 50" W, 1900, F. H. F. Oldenburger & V. V. Meccenas 1881, MO 0720590, 5350, HM010440, HM010459, HM010418; Murillo, La Paz, Bolivia, Bolivia, 16° 39' 22" S, 68° 04' 01" W, 3000, J. C. Solomon & J. Kuijt 11481, MO 0723596, 5330, HM010436, HM010455, HM010414; Santa Cruz, Santa Cruz, Bolivia, 17° 46' 46" S, 63° 13' 22" W, 420, G. Navarro Sánchez 1433, MO 3087777, 5349, HM010439, HM010458, HM010420; Minas Gerais, Minas Gerais, Brazil, 18° 50' 30" S, 48° 21' 31" W, 780, G. M. Feep et al. 432, MO 3085141, 5325, HM010434, missing, HM010412; Boqueron, Boqueron, Paraguay, 21° 40' 11" S, 61° 05' 34" W, 300, F. Merelles & R. Degen 5601, MO 3086819, 5345, HM010437, HM010456, HM010415; Boqueron, Boqueron, Paraguay, 22° 13' 53" S, 60° 23' 48" W, 150, R. Degen & F. Merelles 3168, MO 3085186, 5346, HM010438, HM010457, HM010416; Tapia, Tucuman, Argentina, 26° 35' 51" S, 65° 16' 50" W, 720, G. C. Amico & R. Vidal Russell 240, BCRU*, 5548, HM010441, HM010447, HM010419; Jaquirana, Rio Grande do Sul, Brazil, 28° 51' 08" S, 50° 20' 38" W, 850, R. Wasum et al., MA 473288, 5318, HM010431, HM010451, Missing; Colonia Pellegrini, Corrientes, Argentina, 29° 42' 28" S, 57° 07' 24" W, 65, G. C. Amico & R. Vidal Russell 245, BCRU*, 5550,

HM010443, missing, HM010421; Bonpland, Corrientes, Argentina, 29° 51' 27" S, 57° 30' 09" W, 65, G. C. Amico & R. Vidal Russell 266, BCRU*, 5551, HM010444, missing, HM010422; Lavras do Sul, Rio Grande do Sul, Brazil, 30° 54' 32" S, 53° 58' 09" W, 400, R. R. Brooks, et al. 365, MO 1060778, 5326, HM010435, HM010454, HM010413.

T. belmirensis Roldán & Kuijt: Antioquia, Antioquia, Colombia, 6° 34' 48" N, 75° 31' 48" W, 2,400, R. Fonnegra et al. 5400, HUA*, 5050, HM010427, HM010449, HM010406.

T. flagellaris Tiegh.: Felipe Yofre, Corrientes, Argentina, 29° 05' 52" S, 58° 19' 53" W, 70, G. C. Amico & R. Vidal Russell 243, BCRU*, 5549,

HM010442, missing, HM010420; Los Conquistadores, Entre Ríos, Argentina, 30° 26' 49" S, 58° 23' 38" W, 75, G. C. Amico & R. Vidal Russell 279, BCRU*, 5552, HM010445, missing, HM010423; Carlos Paz, Córdoba, Argentina, 31° 29' 49" S, 64° 34' 30" W, 830, G. C. Amico & R. Vidal Russell 283, BCRU*, 5553, HM010446, missing, HM010424; Chacras, San Luis, Argentina, 32° 34' 23" S, 65° 46' 35" W, 1100, G. C. Amico 187, BCRU*, 5210, HM010429, HM010450, HM010408; El Volcan, San Luis, Argentina, 33° 14' 58" S, 66° 10' 55" W, 970, G. C. Amico 197, BCRU*, 5211, HM010430, HM010450, HM010410; Juana Koslay, San Luis, Argentina, 33° 17' 43" S, 66° 17' 10" W, 785, G. C. Amico 172, BCRU*, 5204, HM010428, HM010450, HM010407.